Pharmaceutical Research, Vol. 23, No. 5, May 2006 (© 2006)
DOI: 10.1007/s11095-006-0026-y

Short Communication

Biopharmaceutical Characterization of the Telomerase Inhibitor BRACO19

S. Taetz,[1] C. Baldes,[1] T. E. Mürdter,[2] E. Kleideiter,[2] K. Piotrowska,[2] U. Bock,[3] E. Haltner-Ukomadu,[3] J. Mueller,[3] H. Huwer,[4] U. F. Schaefer,[1] U. Klotz,[2] and C.-M. Lehr[1,5]

Received November 18, 2005; accepted January 11, 2006

Purpose. To characterize the telomerase inhibitor and G-quadruplex stabilizing substance 9-[4-(*N*,*N*-dimethylamino)phenylamino]-3,6-bis (3-pyrrolodino-propionamido) acridine × 3HCl (BRACO19) in terms of biopharmaceutical properties such as solubility, protein binding, interaction with membrane lipids, cytotoxicity, and permeability across pulmonary epithelial cells.
Methods. Protein binding and interaction with membrane lipids were investigated by two high-performance liquid chromatography methods with immobilized human serum albumin and immobilized phosphatidylcholine, respectively. Cytotoxicity (methyl–thiazolyl–tetrazolium assay) and transport studies were performed with the bronchial cell lines 16HBE14o$^-$ and Calu-3, primary human alveolar epithelial cells, and the intestinal cell line Caco-2. Transport experiments were also done in the presence of cyclosporin A (10 μM) and tetraethylammonium chloride (5 mM) and at low temperature (4°C).
Results. BRACO19 has good solubility of at least 2 mg/mL in water and in physiological buffers of pH 7.4 and below. Protein binding to human serum albumin was 38%. No interaction with membrane lipids could be found. Cytotoxicity in 16HBE14o$^-$, Calu-3, and human alveolar epithelial cells was in the range of IC_{50} = 3.5 to 13.5 μM. Caco-2 cells were not affected at concentrations up to 50 μM. No transport of BRACO19 was detected across either cell monolayer in absorptive direction. In secretory direction, permeability was very low, with P_{app} values in the range of 0.25×10^{-7} to 0.98×10^{-7} cm/s for all epithelial cell cultures tested. The transport was not influenced by cyclosporin A or tetraethylammonium chloride or at 4°C, indicating that no efflux/influx systems or active transport are involved.
Conclusions. From these results, we conclude that the very poor permeability of BRACO19 is its main biopharmaceutical limitation. Further applications will require a suitable formulation to warrant adequate delivery across cellular barriers.

KEY WORDS: cytotoxicity; permeability; protein binding; pulmonary epithelial cells; transport.

INTRODUCTION

Telomerase, a ribonucleoprotein enzyme that belongs to the class of reverse transcriptases, plays an important role in the control of proliferation and carcinogenesis by maintaining the length of telomeres. Telomeres are lasso-like structures at the end of chromosomes. They protect them from recombination, nuclease degradation, DNA repair mechanisms, and end-to-end fusions. They also act as a kind of "mitotic clock" by constant erosion after each cell cycle. Reaching a critical length is a signal for the cell to stop dividing and enter the state of replicative senescence (M1 stage). Cells that bypass replicative senescence and continue dividing will face serious DNA damages and, subsequently, cell death, due to further telomere shortening (M2 stage or crisis). However, cells expressing high levels of telomerase, like cancer cells, can escape this mechanism by keeping the telomere length above this limit and, therefore, by dividing indefinitely (1,2).

The approach of telomerase inhibition for the treatment of cancer attracted an increasing amount of interest in the last few years because telomerase is expressed in most types of cancer cells but not in normal cells, with the exception of hematopoietic stem cells, germ cells, and stem cells of the intestine and the skin.

Non-small cell lung cancer (NSCLC) is the most common form of lung cancer and has a poor prognosis. Misawa *et al.* showed that telomerase inhibition in the NSCLC cell line A549 led to an increase in apoptosis and higher sensitivity to chemotherapeutic agents (3). Inhibiting telomerase with suitable drugs would ideally affect cancer cells only and spare healthy tissue. Due to such inherent

[1] Saarland University, Biopharmaceutics and Pharmaceutical Technology, P.O. Box 15 11 50, 66041 Saarbrücken, Germany.
[2] Dr. Margarete Fischer-Bosch Institute of Clinical Pharmacology, Stuttgart, Germany.
[3] Across Barriers GmbH, Science Park Saar, Saarbrücken, Germany.
[4] SHG Kliniken Völklingen, Center for Heart and Thoracic Surgery, Völklingen, Germany.
[5] To whom correspondence should be addressed. (e-mail: lehr@mx.uni-saarland.de)

ABBREVIATIONS: AB, apical to basolateral (transport/direction); BA, basolateral to apical (transport/direction); hAEpC, primary human alveolar epithelial cells; HSA, human serum albumin; IAM, immobilized artificial membrane; NSCLC, non-small cell lung cancer; P-gp, P-glycoprotein; TEAC, tetraethylammonium chloride.

selectivity, an inhalative application of telomerase inhibitors might be possible. The drug could be delivered directly to the lung, thereby further reducing unwanted systemic drug effects.

A screening for potential telomerase inhibitors led us to the acridine derivative 9-[4-(*N*,*N*-dimethylamino)phenylamino]-3,6-bis (3-pyrrolodino-propionamido) acridine × 3HCl (BRACO19; Fig. 1) (4). This substance inhibits telomerase activity and can lead to telomere dysfunction by G-quadruplex stabilization in telomeres (5,6).

For the development of a new drug formulation, knowledge about biopharmaceutical properties like solubility, cytotoxicity, permeation of the drug across biological barriers (like the lung epithelia), or protein binding is as important as the cytotoxic or pharmacological properties of the drug.

Protein binding and interaction with membrane lipids were tested by two high-performance liquid chromatography (HPLC) methods using immobilized human serum albumin (HSA) and immobilized artificial membrane (IAM) chromatography, respectively.

To investigate the permeability of BRACO19 across relevant biological barriers, we used the SV40 virus immortalized cell line 16HBE14o$^-$ (7,8) and the adenocarcinoma cell line Calu-3 (9,10) as models of the bronchial epithelium. The alveolar epithelium was represented by primary human alveolar type II cells, which develop type I characteristics when cultivated under appropriate conditions (11,12). For comparison, we also included the intestinal adenocarcinoma cell line Caco-2, an established model for intestinal drug absorption (13).

MATERIALS AND METHODS

Substances and Buffers

BRACO19 was synthesized by ENDOTHERM GmbH (Saarbruecken, Germany) according to Harrison *et al.* (14). Identity was proven by nuclear magnetic resonance (NMR), whereas purity was proven by HPLC. Propranolol–HCl was purchased from Synopharm GmbH & Co. KG (Barsbuettel, Germany), cyclosporin A was purchased from Calbiochem® (Merck Bioscience GmbH, Bad Soden, Germany), and fluorescein-Na and tetraethylammonium chloride (TEAC) were obtained from Fluka Chemie GmbH (Buchs, Switzerland).

Hank's balanced salt solution (HBSS) buffer was composed of 137.0 mM NaCl, 5.36 mM KCl, 4.26 mM $NaHCO_3$, 0.18 mM $Na_2HPO_4 \times 7\ H_2O$, 0.44 mM KH_2PO_4, 5.55 mM glucose, 10.0 mM *N*-[2-hydroxyethyl]piperazine-*N*′-[2-ethanesulfonic acid] (HEPES), 0.13 mM $CaCl_2 \times 2\ H_2O$, 0.05 mM $MgCl_2 \times 6\ H_2O$, and 0.04 mM $MgSO_4 \times 7\ H_2O$. For transport experiments, 0.25% bovine serum albumin (BSA; Sigma-Aldrich Chemie GmbH, Taufkirchen, Germany) was added to the HBSS buffer (HBSS/BSA buffer).

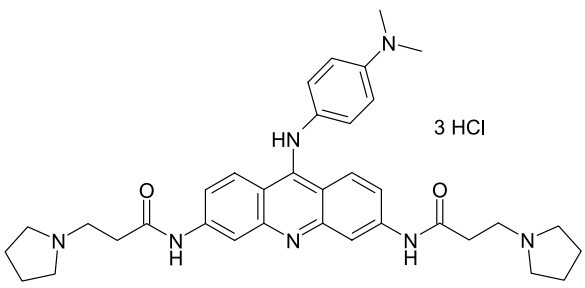

Fig. 1. The 3,6,9-substituted acridine derivative 9-[4-(*N*,*N*-dimethylamino)phenylamino]-3,6-bis(3-pyrrolodinopropionamido) acridine × 3HCl (BRACO19) according to (5).

Sterile balanced salt solution (BSS) contained 137.0 mM NaCl, 5.0 mM KCl, 0.7 mM $Na_2HPO_4 \times 7\ H_2O$, 1.2 mM $MgSO_4 \times 7\ H_2O$, 5.5 mM glucose, 10.0 mM HEPES, 0.18 mM $CaCl_2$, 100 units/mL penicillin, and 100 μg/mL streptomycin. All reagents were of cell culture grade. The pH was adjusted to 7.4 with 1 M NaOH.

Cells and Cell Culture Conditions

Calu-3 cells (HTB-55, ATCC, Manassas, VA, USA) were cultivated in Minimum Essential Medium (MEM), with Earl's salts and L-glutamine (PAA Laboratories GmbH, Pasching, Austria) supplemented with 10% fetal calf serum (FCS), 1% MEM nonessential amino acid (NEAA) solution, and 1 mM sodium pyruvate (all from Sigma-Aldrich).

16HBE14o$^-$ cells were a gift from Dr. Dieter Gruenert (Department of Medicine, University of Vermont, Burlington, VT, USA). They were grown in MEM with Earl's salts and L-glutamine (PAA Laboratories GmbH) supplemented with 10% FCS, 1% NEAA solution, and 3 mM glucose (Sigma-Aldrich).

Caco-2 cells (C2BBe1, ATCC) were cultivated in Dulbecco's Modified Eagle's Medium (DMEM) with high glucose (4.5 g/mL) and L-glutamine (PAA Laboratories GmbH) supplemented with 10% FCS and 1% NEAA solution.

All cell lines were kept in 5% CO_2 and 90–98% humidity at 37°C.

For transport studies, Calu-3 (passages 27 and 32), 16HBE14o$^-$ (passage 2.68), and Caco-2 (passage 83) cells were seeded at a density of 60,000 cells/cm^2 on Transwell® polyester (PET) filter inserts with a growth area of 1.13 cm^2 and a pore size of 0.4 μm (Transwell® Permeable Supports, Corning Inc., NY, USA).

Primary human alveolar epithelial cells (hAEpC) were isolated from nontumor lung tissue of patients undergoing partial lung resection according to Elbert *et al.* (11) with slight modifications of the enzymatic digestion and cell purification (15). In brief, the chopped tissue was digested using a combination of 150 mg trypsin type I (Sigma) and 3 mg elastase (Worthington Biochemical Corp., Lakewood, NJ, USA) in 30 mL BSS for 40 min at 37°C. The AT II cell population was purified by a combination of differential cell attachment, Percoll density gradient centrifugation, and positive selection of epithelial cells with magnetic beads [human anti-HEA (Ep-CAM) MicroBeads, Miltenyi Biotec, Bergisch Gladbach, Germany]. Cell viability was assessed by trypan blue staining.

The isolated hAEpC were seeded at a density of 600,000 cells/cm^2 on collagen/fibronectin-coated Transwell® PET filter inserts (Corning Inc.) with a growth area of 0.33 cm^2. They were grown in saline–adenine–glucose–mannitol (SAGM) medium (Cambrex BioScience Walkersville Inc., Walkersville, MD, USA) supplemented with 1% FCS, 100 units/mL penicillin, and 100 μg/mL streptomycin (Sigma-Aldrich).

The formation of confluent monolayers and tight junctions was verified by measuring the transepithelial electrical resistance (TEER) using an epithelial voltohmmeter (EVOM, World Precision Instruments, Berlin, Germany) with an STX-2 electrode.

For transport experiments, Calu-3 cells were used 14 days post seeding; 16HBE14o$^-$ cells and Caco-2 cells were used after 7 and 21 days, respectively. hAEpC were cultivated for 8 days. TEER values were as reported before or higher for transport experiments (11,16): about 1000 $\Omega \times cm^2$ for Calu-3, 800 $\Omega \times cm^2$ for 16HBE14o$^-$, 750 $\Omega \times cm^2$ for Caco-2, and 1400 $\Omega \times cm^2$ for hAEpC.

Transport Studies

Prior to transport experiments, cell culture media were removed and the apical and basolateral compartments were washed twice with HBSS/BSA buffer. Cells were equilibrated for 2–2.5 h with this buffer.

After the equilibration period, buffer was exchanged with drug solutions of the same buffer in either the apical or basolateral compartment. The volumes for the apical and basolateral side for 16HBE14o$^-$, Calu-3, and Caco-2 were 500 and 1500 μL, respectively. The volumes for hAEpC were 200 μL for the apical side and 800 μL for the basolateral side.

Fifty-microliter samples from the donor compartments were drawn immediately at the beginning and at the end of the transport experiments. Fifty-microliter samples from the acceptor compartments were drawn after 30, 60, 120, 180, 240, and 300 min. An equal volume of fresh buffer was returned to the acceptor compartment after each sampling. The filter plates were kept under cell culture conditions and were slightly shaken with an orbital shaker. TEER values were measured after the equilibration period and at the end of transport experiments to verify that the barrier function of the monolayers was not compromised. The drug concentrations in the donor compartments were as follows: 16HBE14o$^-$: 20 μg/mL of propranolol, fluorescein, and BRACO19, respectively; Calu-3 and Caco-2: 20 μg/mL fluorescein, 100 and 200 μg/mL BRACO19; hAEpC: 100 and 200 μg/mL BRACO19.

Each experiment was performed 5-fold in either direction.

Transport Experiments with Different Inhibitors

Calu-3 cells are known to express the P-glycoprotein (P-gp) efflux system (17) and organic cation transporter proteins (influx/efflux of organic cations) (16). Inhibition of BRACO19 transport was studied at a donor concentration of 200 μg/mL as described in "Transport Studies" with the following modifications. For the inhibition of P-gp and other multidrug resistance efflux systems, we added 10 μM cyclosporin A (18) to the HBSS/BSA buffer. For the inhibition of organic cation transporter proteins, the buffer was supplemented with 5 mM TEAC (19). The inhibitors were present in both compartments. Transport experiments were also performed at 4°C to check for other active transport mechanisms as well as at 37°C without inhibitors for comparison. The results were compared with those of the previous experiments with Calu-3 cells.

Calculation of Apparent Permeability Coefficient P_{app}

The apparent permeability coefficient P_{app} was calculated according to the formula:

$$P_{app}(cm/s) = \frac{J}{A \cdot C_0} \quad (1)$$

where J is the linear section of the flux (micrograms per second), A is the filter area (square centimeters), and C_0 is the initial donor concentration (micrograms per cubic centimeter).

Determination of Uptake into Cells and Adsorption to Filter Material

For adsorption/uptake studies, filters were washed twice with HBSS buffer after the transport experiments and the filter membranes with cells were cut out. Cells were lysed in 1 mL of an 80:20 mixture of methanol/HBSS (v/v) by means of ultrasonication for 30 min. For removal of cell fragments, the suspensions were first kept at −80°C for 45 min and were then centrifuged for 20 min at 14,000 rpm and 0°C. An aliquot of the supernatant was used for analysis.

Sample Analysis

BRACO19 and propranolol samples were analyzed by reversed-phase HPLC using an isocratic Dionex HPLC system consisting of an ASI 100 automated sample injector, UVD 340U diode array detector, and P680 pump with Chromeleon® software (version 6.60 SP1 build 1449; Dionex, Idstein, Germany).

For BRACO19 analysis, a Gemini® RP-18 column (150 × 4.6 mm/5 μm/110 Å) (Phenomenex, Aschaffenburg, Germany) was used. The mobile phase was composed of 80:20 (v/v) methanol/borate buffer pH 10.0 (100 mM). At a flow rate of 0.6 mL/min, the retention time of BRACO19 was 8.9 ± 0.2 min. The UV detector was set at 268 nm.

Propranolol was analyzed with a Lichrospher® RP-18 column (125 × 4 mm/5 μm) (Merck, Darmstadt, Germany). The mobile phase was composed of 45:33:22 (v/v/v) water/methanol/acetonitrile supplemented with 0.033% (v/v) triethylamine and 0.044% (v/v) phosphoric acid. The flow rate was set to 1.2 mL/min, and the retention time was 2.9 ± 0.25 min. Propranolol was detected at 215 nm.

Injection volumes for both substances were 20 μL per sample.

Fluorescein was analyzed by fluorimetry using a Cytofluor II fluorescence reader with Cytofluor software version 4.2 (PerSeptive Biosystems, Wiesbaden-Norderstedt, Germany). Fifty-microliter samples were diluted to 200 μL with 1 mM NaOH in a 96-well plate. The excitation wavelength was set to 485 nm and the emission wavelength to 530 nm.

All unknown samples were calculated against known standards. Standards were in the range of 0.02–20 μg/mL. If necessary, samples were diluted 1:10.

IAM Chromatography Measurements

Immobilized artificial membrane chromatography of BRACO19 was performed with a phosphatidylcholine-func-

tionalized column (Regis Technologies, Morton Grove, IL, USA). The mobile phase was composed of potassium buffer pH 6.8 and acetonitrile. A Waters HPLC system W2790 and PDA detector W2996 with Millenium^{32} software (Milford, MA, USA) was used for analysis. The classification of the drug cellular membrane interaction in terms of permeability was performed by the marker molecules uracil (eluting with the injection peak), atenolol (3.07, 50%), ketoprofen (5.55, 92%), carbamazepine (7.64, 70%), and propranolol (11.55, 90%). The values inside the parentheses indicate the k'_{IAM} values for the compounds and the corresponding fraction absorbed according to the Biopharmaceutical Classification System (BCS) (20).

HSA Binding

Human serum albumin binding of BRACO 19 was investigated by using an HSA-functionalized column (Thermo Hypersil) according to a method developed by Across Barriers GmbH. The mobile phase was composed of ammonium acetate buffer pH 7.4 and propanol. An isocratic Waters HPLC system W2690 and dual wavelength detector W2487 with Millenium^{32} software (Milford) was used for analysis. For the classification of drug binding, the following system was established from different literature values: 0–40% for weak, 40–50% for weak/medium, 50–85% for medium, 85–95% for medium/strong, and >95% for strong drug binding to HSA. Substances for calibration were acetaminophen (24% protein binding), carbamazepine (76%), propranolol (90%), and naproxen (99%).

MTT Cytotoxicity Assay

Cytotoxicity of BRACO19 was tested using the methylthiazolyl-tetrazolium (MTT) assay. 16HBE14o$^-$, Calu-3, and Caco-2 cells were grown at a density of 60,000 cells/cm^2 on 96-well Cellstar® tissue culture plates (Greiner Bio-One, Frickenhausen, Germany) for 6 days under cell culture conditions (see above) in 200 μL medium with different concentrations of BRACO19. hAEpC were grown under the same conditions but at a density of 30,000 cells/cm^2. BRACO19 concentrations were in the range of 0–50 μM. Each concentration was tested in quadruplicate. Cell culture medium with or without BRACO19 was changed every other day. After 6 days, the medium was exchanged for 200 μL BRACO19-free medium, and 10 μL of 5 mg/mL MTT solution in phosphate-buffered saline (PBS) was added to each well. After 3.5 h incubation, the medium was removed and the cells were washed with PBS. Two hundred microliters of 100% isopropanol was added to each well, and the plate was left for crystal dissolution on an orbital shaker overnight. Absorption was measured at a wavelength of 550 nm with a UV/Vis reader (SLT Spectra, Tecan Deutschland GmbH, Crailsheim, Germany). Viability of cells treated with BRACO19 was related to cells grown in BRACO19-free medium. The IC_{50} value was determined by nonlinear regression using SigmaPlot® Version 9 (SPSS Inc., Chicago, IL, USA).

RESULTS

Solubility, Cytotoxicity, Protein Binding, and IAM Chromatography Measurements

BRACO19 showed good and rapid solubility of at least 2 mg/mL in distilled water and physiological buffer solutions in a pH range of 2.8–7.4. For transport experiments, we used a 20 mg/mL stock solution in HBSS/BSA buffer (pH 7.4), which was diluted to the desired concentration before each experiment in the same buffer system.

The IC_{50} values found in the MTT cytotoxicity test were as follows: Calu-3, 13.6 ± 3.8 μM; 16HBE14o$^-$, 3.6 ± 1.2 μM; and hAEpC, 6.0 ± 0.4 μM. Interestingly, Caco-2 cells were not affected by BRACO19 concentrations up to 50 μM.

The binding of BRACO19 to HSA was found to be 38%, indicating a weak-to-medium protein binding referring to the reference compounds. By the IAM chromatography measurements, BRACO19 was eluted very early from the column together with the injection peak. This points out a low potential for BRACO19 to overcome barriers like phospholipid membranes.

Transport Experiments

In the first transport experiment, the permeability of BRACO19 was compared with the high-permeability marker propranolol and the low-permeability marker fluorescein in 16HBE14o$^-$ cells. BRACO19 transport was found to be asymmetrical and very low. For the apical-to-basolateral (AB) direction, no transport could be detected at all. In basolateral-to-apical (BA) direction, transport was about 10-fold lower than for fluorescein.

The results for Calu-3, Caco-2, and hAEpC were comparable to those found with 16HBE14o$^-$ cells. Even after increasing the donor concentrations of BRACO19 to 100 and 200 μg/mL to facilitate detection in the receiver com-

Table I. Apparent Permeability Coefficients (P_{app}; centimeters per second × 10^7) of BRACO19 in Comparison with Propranolol and Fluorescein in Different Cell Lines (16HBE14o$^-$, Calu-3, Caco-2), Primary Human Alveolar Epithelial Cells, and Cell-Free Filters

Substance	Initial donor concentration	16HBE14o$^-$		Calu-3		Caco-2		hAEpC	
		A→B	B→A	A→B	B→A	A→B	B→A	A→B	B→A
BRACO19	20 μg/mL	n.d.	0.98 ± 0.23	–	–	–	–	–	–
BRACO19	100 μg/mL	–	–	n.d.	0.25 ± 0.05	n.d.	0.31 ± 0.03	n.d.	0.66 ± 0.07
BRACO19	200 μg/mL	–	–	n.d.	0.32 ± 0.05	n.d.	0.57 ± 0.03	X	X
Fluorescein	20 μg/mL	4.59 ± 0.66	9.59 ± 0.67	1.15 ± 0.18	1.26 ± 0.14	9.46 ± 1.16	8.95 ± 1.35	–	–
Propranolol	20 μg/mL	131.59 ± 7.37	106.51 ± 5.97	–	–	–	–	–	–

n.d., No substance detectable in acceptor compartment; X, high BRACO19 concentrations led to a collapse of monolayer integrity.

Table II. P_{app} Values (centimeters per second $\times 10^7$) of BRACO19 (200 μg/mL Donor Concentration) in Calu-3 Cells Under Normal Conditions, in the Presence of the P-gp Inhibitor Cyclosporin A (10 μM), the Organic Cation Transporter Protein Inhibitor Tetraethylammonium Chloride (TEAC; 5 mM), and at 4°C

Control		Cyclosporin A		TEAC		4°C	
A→B	B→A	A→B	B→A	A→B	B→A	A→B	B→A
n.d.	0.27 ± 0.03	n.d.	0.92 ± 0.10	n.d.	0.31 ± 0.03	n.d.	0.18 ± 0.04

n.d., No substance detectable in acceptor compartment.

partment, no transport could be detected in the AB direction for either cell line. Also, in the BA direction, the apparent permeability coefficients were still lower than the permeability of fluorescein. The results of all transport experiments are summarized in Table I.

Transport experiments with cell-free filters and BRACO19 solution were performed under analogous conditions to look for the influence of the Transwell® system. The P_{app} values were about 100-fold higher than for filters with cells (data not shown), indicating that the permeation through cell-free filters is not rate limiting.

TEER values of all cell monolayers remained stable or even increased slightly during transport studies. Only in the experiment with hAEpC and 200 μg/mL BRACO19 donor concentrations could a strong decrease in TEER to about 200 $\Omega \times cm^2$ be found. This was accompanied by a comparably strong nonlinear increase in BRACO19 concentrations in the respective acceptor compartments.

Experiments with Transport Inhibitors and Uptake/ Adsorption Studies

The results for transport experiments with Calu-3 cells in the presence of different inhibitors are summarized in Table II. They were comparable to those under normal conditions: no transport in the AB direction was detected, and the P_{app} values for the BA transport were within the range of the former experiments. This indicates that efflux/influx systems or active transport is not involved in the transport of BRACO19.

The asymmetry found in the transport experiments could also be observed in the uptake/adsorption studies (Fig. 2). Filters that were in direct contact with BRACO19 solution from the basolateral side (BA transport) contained more BRACO19 than those that were in contact with the solution from the apical side (AB transport). An exception was the transport experiment with hAEpC at 200 μg/mL BRACO19 donor concentration where the integrity of the monolayers collapsed. Here, the amounts of BRACO19 in filters found for the AB transport were similar to those for the BA transport. Amounts of BRACO19 found in cell-free filters treated under the same conditions were comparable to those of BA transport.

DISCUSSION

Our studies showed that BRACO19 has a good solubility in aqueous media in the concentrations that were used. The *in vitro* cytotoxicity of BRACO19 for our pulmonary epithelial cells was comparable to values found in literature for other cancerous cell lines derived from other organs (e.g., vulva carcinoma cells, breast cancer cells, or uterus carcinoma cells) (5,6,21). In comparison to "classic" anticancer drugs, the cytotoxicity of BRACO19 was within the range

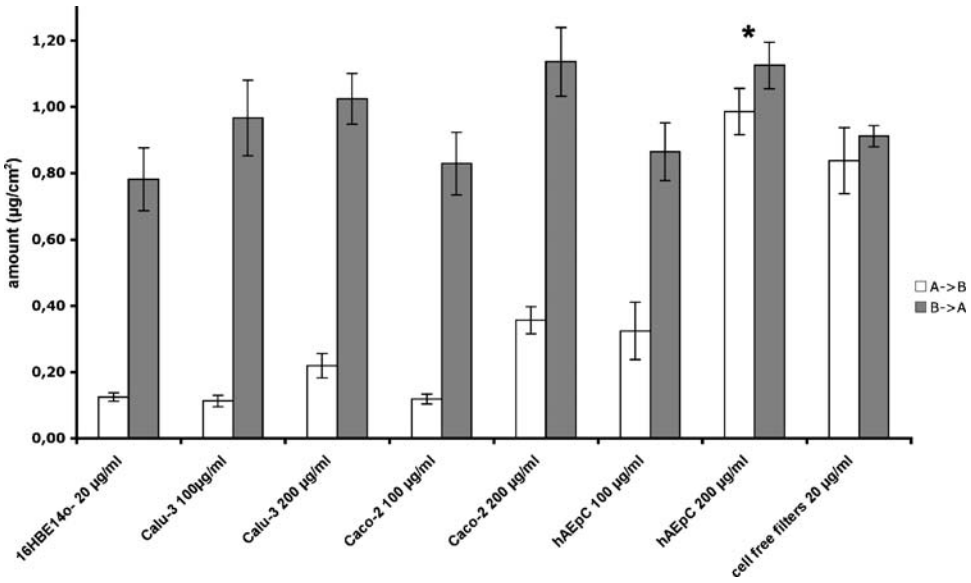

Fig. 2. Amounts of BRACO19 (micrograms per square centimeter) recovered from excised filters. Concentrations refer to initial donor concentration of BRACO19. *Integrity of monolayer compromised by high BRACO19 concentration.

of cisplatin (10–25 μM) (22,23) but lower than for doxorubicin (0.4–2.4 μM) (24), paclitaxel (0.7–1.8 nM) (23), or vincristine (1.9–3.5 nM) (25). However, it has to be kept in mind that the strategy of this therapeutic approach is the (re)induction of senescence and apoptosis by telomerase inhibition (i.e., a controlled cell death) and not the simple poisoning of malignant cells. Therefore, a high IC_{50} value is desired.

Protein binding of BRACO19 to HSA was rather weak compared with reference drugs. The results from IAM chromatography measurements suggest that interaction of BRACO19 with membrane lipids is negligible because there is a proportional relationship between the capacity factor k'_{IAM} and the membrane partitioning coefficient K_m (26).

Our transport studies showed that BRACO19 has to face great problems to overcome biological barriers. The transport experiments with Caco-2 cells, a standard model for intestinal drug absorption, indicate that BRACO19 might not be suitable for oral administration. Burger *et al.* (6) already demonstrated that tumor xenografts in mice did not respond to an oral treatment with BRACO19. Even when BRACO19 was administered intraperitoneally, only early stage tumors and not late stage tumors were susceptible to the medication.

Since the results for the intestinal cell line Caco-2 are comparable to those of our bronchial cell lines 16HBE14o$^-$ and Calu-3, as well as to the primary alveolar cells, hAEpC, we can assume that a topical application, like an inhalative treatment of lung cancer, will face similar problems as the oral route. Although a systemic availability is not needed, BRACO19 has at least to be able to overcome the epithelial (air/blood) barrier to reach deeper regions of a lung tumor. The transport results are confirmed by IAM chromatography measurements because the capacity factor k'_{IAM} can be correlated with the apparent permeability coefficient P_{app} (27).

Also, the concentrations used for the transport experiments are not representative for possible therapeutical applications because they were far above the IC_{50} values of our cells (10 μM ≈ 7 μg/mL). hAEpC were most sensitive to high BRACO19 concentrations in the transport experiments, as could be seen in the strong decrease in TEER at the 200 μg/mL donor concentration. Since the major part of the pulmonary surface belongs to the alveolar region, high drug concentrations would result in unwanted side effects. Lower concentrations, however, would result in even less drug absorption and inefficacy.

The apparent asymmetry in transport can be explained with a relatively strong adsorption to the filter material, as has been demonstrated in the experiments with cell-free filters (Fig. 2). For transport experiments in the BA direction, the filters were rapidly saturated with BRACO19 because they were in direct contact with the solution. Hence, transport was not hindered. However, when BRACO19 was applied from the apical side, the small amounts that permeated across the monolayer were completely adsorbed to the filter material. Since the filter was not saturated at the end of the transport experiment, no substance could be detected in the basolateral compartment. Differences in adsorptions (Fig. 2) were most likely due to varying amounts of BRACO19 adsorbed to surface mucus and proteins (for the AB direction) or entrapped in the intercellular space.

Our observations can be explained by the chemical properties of BRACO19. It contains two basic pyrrolidine rings (Fig. 1) that are very likely to be protonated under physiological conditions; that is, the molecule is positively charged. This results in good water solubility but strongly decreases the interaction with hydrophobic structures like cell membranes. The small amounts that were transported in the BA direction most probably took the paracellular route by passive diffusion because no active transport mechanisms or efflux/influx systems like P-gp or organic cation transporter proteins could be identified. Also, the fact that BRACO19 does not interact with membrane phospholipids and that higher amounts were only detectable in the acceptor compartments and filters after the monolayer integrity collapsed argue for the paracellular way.

CONCLUSION

From our results, we would suggest that BRACO19 has the typical properties of a class III drug substance according to the BCS: a good aqueous solubility and a very poor permeability across biological barriers.

Obviously, BRACO19 is a potent substance with an interesting new mode of action, i.e., telomerase inhibition by G-quadruplex stabilization but with challenging biopharmaceutical properties. Hence, suitable formulations for the efficient delivery of this compound must be developed first to further evaluate this new therapeutical concept.

ACKNOWLEDGMENTS

This project was financially supported by Deutsche Krebshilfe e.V., Bonn, Germany (project no.: 10-2035-Kl I) and by the Robert Bosch Foundation, Stuttgart, Germany.

REFERENCES

1. E. H. Blackburn. Telomeres and telomerase: their mechanisms of action and the effects of altering their functions. *FEBS Lett.* **579**:859 (2005).
2. J. W. Shay and W. E. Wright. Senescence and immortalization: role of telomeres and telomerase. *Carcinogenesis* **26**:867–874 (2005).
3. M. Misawa, T. Tauchi, G. Sashida, A. Nakajima, K. Abe, J. H. Ohyashiki, and K. Ohyashiki. Inhibition of human telomerase enhances the effect of chemotherapeutic agents in lung cancer cells. *Int. J. Oncol.* **21**:1087–1092 (2002).
4. K. Piotrowska, E. Kleideiter, T. E. Mürdter, S. Taetz, C. Baldes, U. Schaefer, C. M. Lehr, and U. Klotz. Optimization of the TRAP assay to evaluate specificity of telomerase inhibitors. *Lab. Invest.* **85**(12):1565–1569 (2005).
5. S. M. Gowan, J. R. Harrison, L. Patterson, M. Valenti, M. A. Read, S. Neidle, and L. R. Kelland. A G-quadruplex-interactive potent small-molecule inhibitor of telomerase exhibiting *in vitro* and *in vivo* antitumor activity. *Mol. Pharmacol.* **61**:1154–1162 (2002).
6. A. M. Burger, F. Dai, C. M. Schultes, A. P. Reszka, M. J. Moore, J. A. Double, and S. Neidle. The G-quadruplex-interactive molecule BRACO-19 inhibits tumor growth, consistent with telomere targeting and interference with telomerase function. *Cancer Res.* **65**:1489–1496 (2005).
7. A. L. Cozens, M. J. Yezzi, K. Kunzelmann, T. Ohrui, L. Chin, K. Eng, W. E. Finkbeiner, J. H. Widdicombe, and D. C. Gruenert. CFTR expression and chloride secretion in polarized immortal

human bronchial epithelial cells. *Am. J. Respir. Cell Mol. Biol.* **10**:38–47 (1994).
8. B. Forbes, A. Shah, G. P. Martin, and A. B. Lansley. The human bronchial epithelial cell line 16HBE14o^{-} as a model system of the airways for studying drug transport. *Int. J. Pharm.* **257**:161–167 (2003).
9. B. I. Florea, M. L. Cassara, H. E. Junginger, and G. Borchard. Drug transport and metabolism characteristics of the human airway epithelial cell line Calu-3. *J. Control. Release* **87**:131–138 (2003).
10. K. A. Foster, M. L. Avery, M. Yazdanian, and K. L. Audus. Characterization of the Calu-3 cell line as a tool to screen pulmonary drug delivery. *Int. J. Pharm.* **208**:1–11 (2000).
11. K. J. Elbert, U. F. Schaefer, H. J. Schafers, K. J. Kim, V. H. Lee, and C. M. Lehr. Monolayers of human alveolar epithelial cells in primary culture for pulmonary absorption and transport studies. *Pharm. Res.* **16**:601–608 (1999).
12. S. Fuchs, A. J. Hollins, M. Laue, U. F. Schaefer, K. Roemer, M. Gumbleton, and C. M. Lehr. Differentiation of human alveolar epithelial cells in primary culture: morphological characterization and synthesis of caveolin-1 and surfactant protein-C. *Cell Tissue Res.* **311**:31–45 (2003).
13. P. Artursson, K. Palm, and K. Luthman. Caco-2 monolayers in experimental and theoretical predictions of drug transport. *Adv. Drug Deliv. Rev.* **46**:27–43 (2001).
14. R. J. Harrison, J. Cuesta, G. Chessari, M. A. Read, S. K. Basra, A. P. Reszka, J. Morrell, S. M. Gowan, C. M. Incles, F. A. Tanious, W. D. Wilson, L. R. Kelland, and S. Neidle. Trisubstituted acridine derivatives as potent and selective telomerase inhibitors. *J. Med. Chem.* **46**:4463–4476 (2003).
15. C. Ehrhardt, K. J. Kim, and C. M. Lehr. Isolation and culture of human alveolar epithelial cells. *Methods Mol. Med.* **107**:207–216 (2005).
16. C. Ehrhardt, C. Kneuer, C. Bies, C. M. Lehr, K. J. Kim, and U. Bakowsky. Salbutamol is actively absorbed across human bronchial epithelial cell layers. *Pulm. Pharmacol. Ther.* **18**: 165–170 (2005).
17. K. O. Hamilton, G. Backstrom, M. A. Yazdanian, and K. L. Audus. P-glycoprotein efflux pump expression and activity in Calu-3 cells. *J. Pharm. Sci.* **90**:647–658 (2001).
18. M. Qadir, K. L. O'Loughlin, S. M. Fricke, N. A. Williamson, W. R. Greco, H. Minderman, and M. R. Baer. Cyclosporin A is a broad-spectrum multidrug resistance modulator. *Clin. Cancer Res.* **11**:2320–2326 (2005).
19. H. Koepsell, B. M. Schmitt, and V. Gorboulev. Organic cation transporters. *Rev. Physiol., Biochem. Pharmacol.* **150**:36–90 (2003).
20. U. Bock, T. Flototto, and E. Haltner. Validation of cell culture models for the intestine and the blood–brain barrier and comparison of drug permeation. *ALTEX* **21**(Suppl 3):57–64 (2004).
21. C. M. Incles, C. M. Schultes, H. Kempski, H. Koehler, L. R. Kelland, and S. Neidle. A G-quadruplex telomere targeting agent produces p16-associated senescence and chromosomal fusions in human prostate cancer cells. *Mol. Cancer Ther.* **3**: 1201–1206 (2004).
22. M. Loprevite, R. E. Favoni, A. de Cupis, P. Pirani, F. Merlo, F. Grossi, and A. Ardizzoni. Pre-clinical evaluation of new anti-neoplastic agents in NSCLC cell lines: evidence of histological subtype-dependent cytotoxicity. *Int. J. Oncol.* **15**:787–792 (2004).
23. J. A. Smith, H. Ngo, M. C. Martin, and J. K. Wolf. An evaluation of cytotoxicity of the taxane and platinum agents combination treatment in a panel of human ovarian carcinoma cell lines. *Gynecol. Oncol.* **98**:141–145 (2005).
24. R. Ravizza, M. B. Gariboldi, L. Passarelli, and E. Monti. Role of the p53/p21 system in the response of human colon carcinoma cells to doxorubicin. *BMC Cancer* **4**:92 (2004).
25. S. Kobayashi, S. Okada, H. Yoshida, and S. Fujimura. Indomethacin enhances the cytotoxicity of VCR and ADR in human pulmonary adenocarcinoma cells. *Tohoku J. Exp. Med.* **181**: 361–370 (1997).
26. S. Ong, H. Liu, X. Qiu, G. Bhat, and C. Pidgeon. Membrane partition coefficients chromatographically measured using immobilized artificial membrane surfaces. *Anal. Chem.* **67**:755–762 (1995).
27. C. Pidgeon, S. Ong, H. Liu, X. Qiu, M. Pidgeon, A. H. Dantzig, J. Munroe, W. J. Hornback, J. S. Kasher, and L. Glunz. IAM chromatography: an *in vitro* screen for predicting drug membrane permeability. *J. Med. Chem.* **38**:590–594 (1995).